## **Comparison of Coherent and Incoherent Donut Beams for Deep Tissue STED Microscopy**

Thariq Shanavas, Robert R. McLeod, Mark E. Siemens, and Juliet T. Gopinath 1,2,4,\*

<sup>1</sup>Department of Physics, University of Colorado, Boulder, CO 80309, USA
<sup>2</sup>Department of Electrical, Computer and Energy Engineering, University of Colorado, Boulder, CO 80309, USA
<sup>3</sup>Department of Physics, University of Denver, Denver, CO 80204

<sup>4</sup>Materials Science Engineering Program, University of Colorado, Boulder, CO 80309, USA

\*julietg@colorado.edu

**Abstract:** We numerically compare the null quality for STED microscopy generated by Laguerre-Gaussian beams with orbital angular momentum and donut beams generated by incoherent addition of orthogonal Hermite Gaussian beams when imaging deep biological tissue. © 2023 The Author(s)

## 1. Introduction

Stimulated emission depletion (STED) microscopy has proven to be a powerful imaging technique that offers a sub-diffraction limited resolution. In STED microscopy, a fluorescence excitation beam is overlapped with a spatially structured depletion beam [1]. The depletion beam has a donut shape with a minimum at the center and is tuned to the tail of the fluorescence emission spectrum to deplete the fluorescence and create a smaller effective illumination area. The donut beams are typically generated by imparting a spiral phase to a Gaussian beam by passing it through a spiral phase plate or a spatial light modulator.

Fiber-based delivery of STED excitation and depletion beams has been proposed in recent years [2]. An obstacle to fiber-based STED for live-animal imaging is that commercially available step index fiber supports doughnut-shaped modes that are very nearly degenerate. Therefore, perturbations arising from the bending of the fiber transfer power from one mode to another, which then interfere to produce a beam with no central null.

One proposed solution to deliver donut modes to the microscope objective is to couple temporally incoherent Hermite-Gaussian (HG) modes to the non-degenerate orthogonal axes of a polarization maintaining (PM) fiber. Because of temporal incoherence, the two modes do not interfere at the objective and deliver a donut shaped beam regardless of the relative phase accumulated between the two modes due to bend in the fiber [1] [Fig. 1]. Such a donut beam carries no orbital angular momentum (OAM).

a donut beam carries no orbital angular momentum (OAM).

There have been reports of self-healing properties of beams with OAM in obstructed media [3] and deeper penetration depth

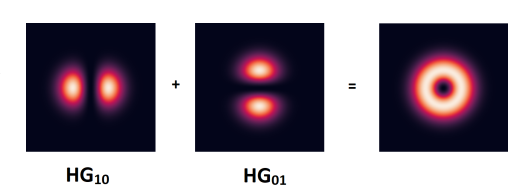


Fig. 1: Incoherently adding the  $HG_{10}$  and  $HG_{01}$  eigenmodes of a PM fiber produces a donut beam with the same spatial profile as an  $LG_{01}$  beam.

in tissue as compared to non-OAM beams [4]. This naturally raises the question of whether incoherent donut beams maintain the vortex null as well as Laguerre-Gaussian (LG) beams with OAM inside the highly scattering biological tissue. In this work, we employ the Fourier beam propagation algorithm to simulate both LG beams with OAM and the incoherent donut from two HG beams. We also estimate how the quality of the vortex null deteriorates as we image deeper into tissue.

## 2. Methods and Inferences

The scattering properties of biological tissue are captured by the scattering mean free path ( $l_s$ ) and the anisotropy factor (g). Following the experimental results of Ding et al. [5], we simulated a scattering medium with  $l_s$  = 15 µm and g = 0.92 corresponding to mouse brain tissue at 500 nm. We use the method outlined by Cheng et al. [6] to generate a 3-dimensional matrix representing the refractive index with fluctuations corresponding to the required mean free path and anisotropy factor. We used the Fourier beam propagation technique with a lateral resolution of 83 nm and an axial resolution of 500 nm to simulate the beam profile at various tissue depths from 5 µm to 150 µm. The beam was focused into tissue with a water immersion objective. We start with a low numerical aperture objective of 0.13 NA as an intermediate step and plan to extend our results in the future to the tight focusing case

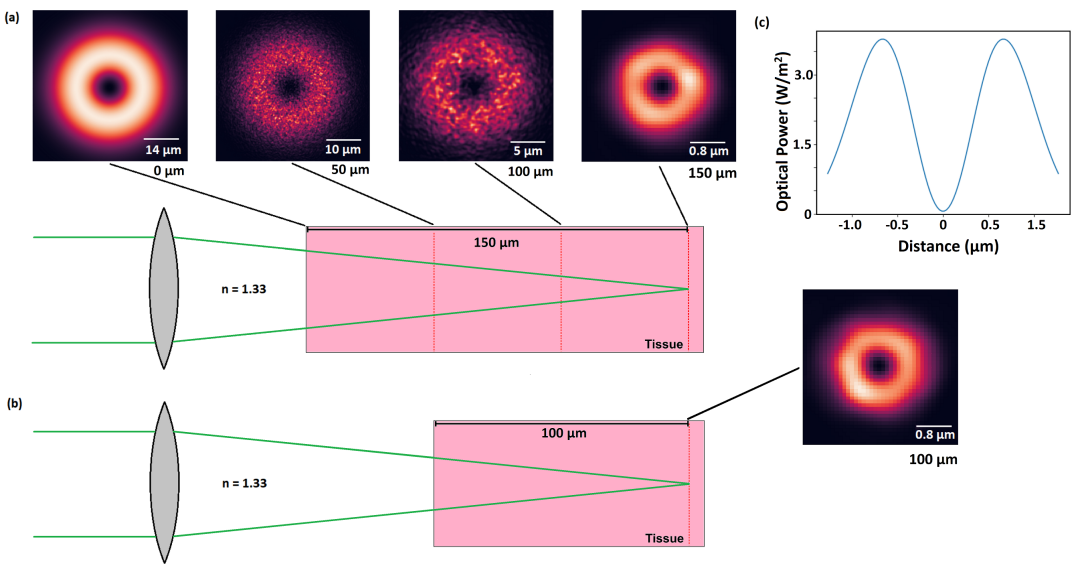
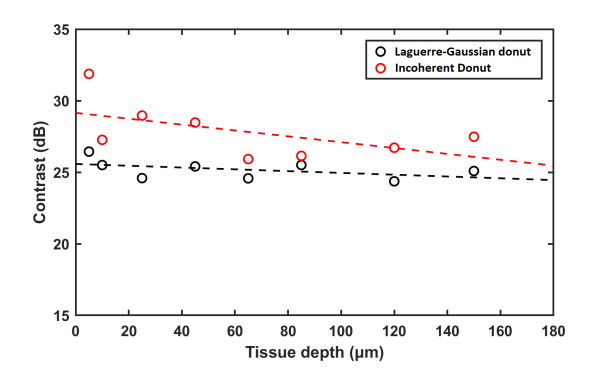


Fig. 2: Spatial profile of an  $LG_{01}$  beam as it is focused (a) 150  $\mu$ m (b) 100  $\mu$ m into tissue. The numerical aperture of the objective is fixed to ensure the spot size remains constant as the tissue depth is varied. The tissue is index-matched using a water immersion. (c) Averaged intensity across 20 cross-sections at various angles in the focal plane of an LG beam focused 150  $\mu$ m deep in tissue. The peak intensity is about 600 nm from the null.

appropriate for STED. The beam profile at various depths for a beam focused 150  $\mu$ m into tissue is shown in Fig. 2(a). We also show the focal plane beam profile for 100  $\mu$ m tissue depth in Fig. 2(b).

The quality of the vortex nulls of the LG beams and the incoherent donut beams were characterized by the contrast between the central null and the peak intensity of the beam. The contrast was measured by taking the average across 20 cross-sections at various angles [Fig. 2(c)]. The deterioration of the vortex null with tissue penetration presented in Fig.3 was calculated by averaging the contrast across 50 instantiations of random tissue samples with the same  $l_s$  and g. The contrast between the null and the peak field is about 28 dB for both types of beams at 5 µm tissue penetration and falls with depth. We expect, that if we refine our simulation to include nonlinear loss, the contrast will deteriorate faster with depth, and that both types of beams will experience a similar effect. Hence, we conclude that there would be no significant advantage to using LG beams for STED microscopy over incoherent donut beams in the limit of a low-NA objective and negligible nonlinear loss. This is an important finding for tissue imaging with STED. We plan to extend this study to tight focusing and nonlinear loss in the future.



**Fig. 3:** Contrast of the central null vs depth for Laguerre-Gaussian beams and incoherent donut beams averaged over 50 simulation runs. The contrast is highest near the surface at about 28 dB and falls with tissue depth. Both types of beams have comparable quality for a given depth and the difference is within the spread of observed values.

## References

- 1. B. M. Heffernan, S. A. Meyer, D. Restrepo, M. E. Siemens, E. A. Gibson, and J. T. Gopinath, "A fiber-coupled stimulated emission depletion microscope for bend-insensitive through-fiber imaging," Scientific Reports 9(1), 11,137 (2019).
- 2. W. Zong, R. Wu, M. Li, Y. Hu, Y. Li, J. Li, H. Rong, H. Wu, Y. Xu, Y. Lu, H. Jia, M. Fan, Z. Zhou, Y. Zhang, A. Wang, L. Chen, and H. Cheng, "Fast high-resolution miniature two-photon microscopy for brain imaging in freely behaving mice," Nature Methods 14(7), 713–719 (2017).
- 3. S. Zhao, W. Zhang, L. Wang, W. Li, L. Gong, W. Cheng, H. Chen, and J. Gruska, "Propagation and self-healing properties of Bessel-Gaussian beam carrying orbital angular momentum in an underwater environment," Scientific Reports 9(1), 2025 (2019).
- 4. N. Biton, J. Kupferman, and S. Arnon, "OAM light propagation through tissue," Scientific Reports 11(1), 2407 (2021).
- 5. H. Ding, F. Nguyen, S. A. Boppart, and G. Popescu, "Optical properties of tissues quantified by Fourier-transform light scattering," Optics Letters **34**(9), 1372–1374 (2009).
- X. Cheng, Y. Li, J. Mertz, S. Sakadžić, A. Devor, D. A. Boas, and L. Tian, "Development of a beam propagation method
  to simulate the point spread function degradation in scattering media," Optics Letters 44(20), 4989–4992 (2019).